

Neurosymbolic artificial intelligence via large language models and coherence-driven inference

Steve Huntsman
and Jewell Thomas

STEVE.HUNTSMAN@CYNNOVATIVE.COM
JEWELL.THOMAS@CYNNOVATIVE.COM

Abstract

We devise an algorithm to generate sets of propositions that objectively instantiate graphs that support coherence-driven inference. We then benchmark the ability of large language models (LLMs) to reconstruct coherence graphs from (a straightforward transformation of) propositions expressed in natural language, with promising results from a single prompt to models optimized for reasoning. Combining coherence-driven inference with consistency evaluations by neural models may advance the state of the art in machine cognition.

1. Introduction

Classical *coherence-driven inference* (CDI) (Thagard and Verbeurgt, 1998; Thagard, 2002; Blokpoel and van Rooij, 2024) models many forms of cognition as solving a constraint satisfaction problem. In this approach, propositions and their consistency relations are encoded in a weighted graph G as in Figure 1. Up to an irrelevant constant that varies among formulations, the *coherence* of $U \subseteq V(G)$ is $-\sum_{u \in U, v \notin U} A_{uv}$, where A is the weighted adjacency matrix of G . (As is common in the literature, we often assume $A_{uv} \in \{\pm 1\}$ in this paper; our benchmarking approach handles this case naturally.) The problem of maximizing coherence is thus an instance for the matrix $-A$ of the APX-complete MAX-CUT problem (Khot et al., 2007; Moore and Mertens, 2011; Gärtner and Matousek, 2012; Lee and Xu, 2021). The objective is to cut the most negative weights in G with a bipartition into accepted (= estimated true) and rejected (= estimated false) propositions.¹

CDI is deeply informed by cognitive science, and experimentally validated by psychological case studies, including assessments of legal reasoning (Holyoak and Simon, 1999; Simon, 2004). It is a computationally credible model for causal inference (Thagard, 2004) suited for making decisions about ill-structured problems (Frigotto and Rossi, 2015). Other illustrations of its capacity for high-level reasoning include reaching deliberative consensus (Joseph and Prakken, 2009) and solving normative inconsistencies (Criado et al., 2016), as well as many complementary examples cited in Blokpoel and van Rooij (2024). CDI can also explicitly incorporate ethical considerations and provide explanations of its reasoning (Yilmaz et al., 2017).

However, mechanisms for automatically generating coherence graphs from natural language data have not been developed: coherence graphs have almost always been constructed manually. (A

1. In general, context matters for assigning acceptance and rejection to a computed bipartition. The most common approach is to prioritize data. For example, direct observations and firm prior conclusions carry more weight than secondhand reports and tentative prior conclusions. See Blokpoel and van Rooij (2024) for a discussion of this point and remarks about implementing a data priority scheme in the present context. (Implementing a data priority scheme is straightforward in the more general computational context outlined in §A.2: just introduce appropriately weighted [or “hard”] single-variable clauses into a weighted SAT instance.) A natural criterion *in vacuo* is to prioritize the part of the bipartition whose induced subgraph has greater normalized internal coherence.

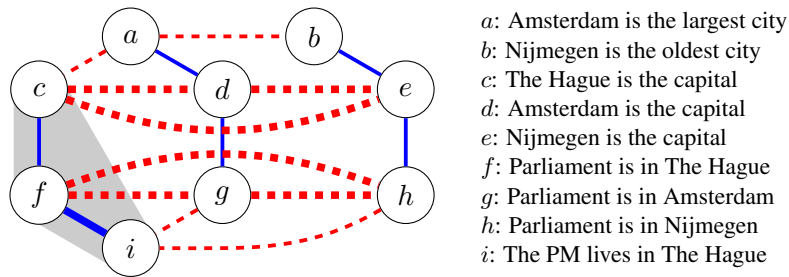


Figure 1: A cartoon of classical coherence, elaborating on an example in Blokpoel and van Rooij (2024). Consistent (solid blue) and inconsistent (red dashed) pairs of vertices (= propositions) respectively get positive and negative weights in a coherence graph, with **magnitude/thickness** indicating the strength of (in)consistency. In this example, the optimal bipartitions are defined by the sets $\{c, f, i\}$ (indicated with a gray vertex cluster), $\{b, c, f, i\}$, $\{b, c, e, f, i\}$, and $\{b, c, e, f, h, i\}$. (It turns out in this particular example that if there are only one or two edge weight magnitudes as indicated, their relative values do not affect any meaningful results due to symmetry.) Near-optimal *Rashomon* solutions (Semenova et al., 2022) such as $\{a, d, f, i\}$ can become optimal if the graph is perturbed.

notable exception is the specialized construction of Joseph and Prakken (2009) using the deduction relation of an underlying logic.) In this paper, we show how to generate a set of propositions in natural language that objectively instantiate a specified coherence graph. We then benchmark the ability of large language models (LLMs) (Brown et al., 2020) to (re)construct coherence graphs, with promising results from a single prompt to models optimized for reasoning: see Figures 4, 5, and 6, as well as Table 1. Another shortcoming of classical CDI that we address in §A.2 is a lack of a natural mechanism for collectively relating three or more propositions, e.g., trilemmas.

A hybrid architecture combining LLMs and CDI naturally separates concerns and is unique in the breadth of straightforward applications. CDI is suited for “slow” or “system 2” reasoning with hard computations performed on impoverished representations (Kahneman, 2011). In contrast, previous neurosymbolic (Sarker et al., 2022; Marra et al., 2024) efforts that use LLMs to help with graph coloring (Khandelwal et al., 2024) or transform natural language data into a logical formula that can be passed to a solver (Olausson et al., 2023; Pan et al., 2023; Ye et al., 2024) reason at a low level of abstraction, cannot resolve ambiguity after the representational process, and can suffer from parsing errors (Feng et al., 2024). Meanwhile, benchmarks appropriate for evaluating the performance of such efforts using propositional or first-order logic (Zhong et al., 2021; Han et al., 2022; Saparov and He, 2023) are not suitable for evaluating coherence.

Meanwhile, transformer-based architectures (Vaswani et al., 2017) like LLMs are suited for “fast” or “system 1” reasoning with easy computations on rich representations (Lenat and Marcus, 2023; Bengio and Malkin, 2024). Transformers are computationally weak without chain-of-thought (CoT) reasoning, but become more powerful with it (Merrill and Sabharwal, 2024). In principle, using CoT linear in input size allows transformers to simulate automata and recognize regular languages, or emulate a probabilistic Turing machine in quasi-quadratic time (Pérez et al., 2021; Nowak et al., 2024). Transformers using polynomial-size CoT can also solve the problems in \mathbf{P} . However, the computation of a transformer with L layers on a prompt of length n can be performed using

$O(L \log n)$ bits of memory under common assumptions. As a corollary, multilayer transformers cannot scalably solve the easy problems 2-SAT or Horn-SAT unless $L = NL$ (Peng et al., 2024). On the other hand, the representational power of multi-head transformer architectures is bounded below by n -gram models (Rajaraman et al., 2024), which perform well in practice (Liu et al., 2024).

The paper is organized as follows. §2 explains how to produce propositions that naturally correspond to a given coherence graph. §3 outlines our experimental setup and §4 details the results of our experiments. We conclude in §5. Appendices respectively give substantial information on generalizing and computing CDI (§A); a case study in which ChatGPT-4 outperformed a skilled human at assigning consistency ratings to proposition pairs (§B); ANOVA (§C); the effects of using different graph-theoretical algorithms in our benchmarking approach (§D); a preliminary mechanistic interpretation of how attention mechanisms may underlie our results (§E); characteristics of the graphs we generated for benchmarking (§F), our prompt template (§G), and finally an alternative fidelity characterization (§H). **We plan to release code and data in the coming weeks.**

2. Modeling coherence graphs

Classical CDI focuses on signed graphs, which approximate more elaborate constructions such as weighted simplicial complexes that may be appropriate for modeling and computing coherence in full generality (for which see Huntsman et al. (2024) and §A.2).

Definition 1 Recall that a signed graph $G_\sigma = (V, E, \sigma)$ is an undirected graph $G = (V, E)$ augmented with a sign map $\sigma : E \rightarrow \{\pm 1\}$. A coherence graph is a signed graph whose vertices are propositions.² Two propositions v and w are dependent in G_σ if $(v, w) \in E$ (in particular, v and w are assumed to be distinct). Two dependent propositions are consistent for σ (resp., inconsistent for σ) if $\sigma(v, w) = +1$ (resp., -1). The left panel of Figure 2 shows an example.

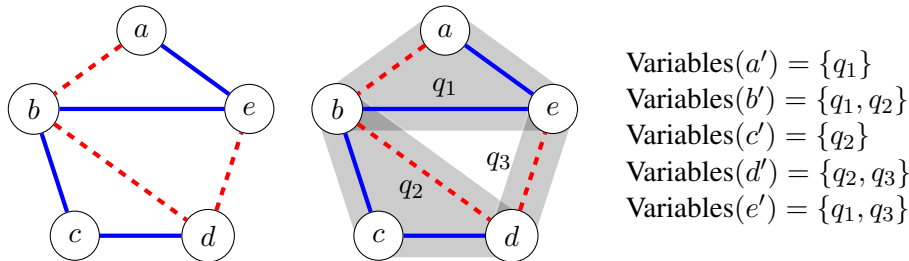


Figure 2: Left: a coherence graph for five propositions $\{a, \dots, e\}$, such that the pairs (a, e) , (b, c) , (b, e) , and (c, d) are consistent (indicated by solid blue edges, and corresponding to edge weights of $+1$); meanwhile, the pairs (a, b) , (b, d) , and (d, e) are inconsistent (indicated by dashed red edges, and corresponding to edge weights of -1). Center: cliques q_1 , q_2 , and q_3 (indicated by gray vertex clusters) yield a minimal clique edge partition (hence cover). Right: each vertex is assigned variables corresponding to the cliques that cover it.

A consistency oracle ε is a function that sends any pair of distinct propositions expressed in natural language to $\{-1, 0, 1\}$. When $\varepsilon(v, w) = -1, 0$, and 1 , v and w are respectively (dependent

2. In practice we can use a more expressive framework than (natural language generation applied to) propositional logic, but we use the term *proposition* throughout; Algorithm 1 involves *bona fide* propositional formulas.

and) inconsistent for ε , independent for ε , and (dependent and) consistent for ε . While LLMs can effectively detect inconsistencies between two propositions (see [Huntsman et al. \(2024\)](#); [Kumar and Roussinov \(2024\)](#), and §B), we will initially restrict consideration to synthetic propositions for which the output of any “reasonable” consistency oracle (i.e., one in which propositions that express logical formulas in natural language are evaluated in the natural way suggested by the underlying formulas) is practically obvious and unambiguous.

Definition 2 Given a consistency oracle ε , a coherence graph $G_\sigma = (V, E, \sigma)$, a set of propositions V' expressed in natural language, and a bijection $\iota : V' \rightarrow V$, we say that V' models G_σ relative to ε and write $V' \models_\varepsilon G_\sigma$ if for all distinct $v', w' \in V'$ we have $\varepsilon(v', w') = \sigma_0(\iota(v'), \iota(w'))$, where σ_0 extends σ to all pairs of distinct propositions in V by taking the value zero on independent pairs.

We will give a general method for constructing $V' \models_\varepsilon G_\sigma$ under any reasonable consistency oracle ε , which we informally write $V' \models G_\sigma$.

For example, taking G_σ to be the coherence graph in the left panel of Figure 2,

$$V' = \{a' : (q_1 \text{ is } p_1), \quad b' : (q_1 \text{ is NOT } p_1 \text{ AND } q_2 \text{ is NOT } p_1), \quad c' : (q_2 \text{ is } p_2), \\ d' : (q_2 \text{ is } p_1 \text{ AND } q_3 \text{ is } p_1), \quad e' : (q_1 \text{ is } p_2 \text{ AND } q_3 \text{ is NOT } p_1)\}$$

where the (clique) variables q_j are placeholders for nouns and the properties p_k are placeholders for gradable (hence negatable) adjectives (e.g., “hot,” “bright,” “loud,” etc.) and $\iota : a' \mapsto a, \dots, e' \mapsto e$, we can see that $V' \models G_\sigma$. A structurally equivalent model $V'' \models G_\sigma$ is

$$V'' = \{a'' : (\text{the living room is hot}), \quad b'' : (\text{the living room is cold and the kitchen is cold}), \\ c'' : (\text{the kitchen is bright}), \quad d'' : (\text{the kitchen is hot and the bedroom is hot}), \\ e'' : (\text{the living room is bright and the bedroom is cold})\}.$$

While there are structurally inequivalent sets of propositions that model G_σ , a set of the form above is extremal in that its clique edge cover and star forest decomposition are minimal: see §2.1.

2.1. An algorithm for modeling coherence graphs

Here we detail how to construct a set of propositions that model a coherence graph.

Definition 3 A clique edge cover of a graph G ([Erdős et al., 1966](#); [Gross et al., 2018](#); [Conte et al., 2020](#)) is a set of cliques in G whose edges cover $E(G)$. A star forest decomposition of G ([Akiyama and Kano, 1985](#); [Kottarathil et al., 2024](#)) is a partition of $E(G)$ into star forests, i.e., forests whose connected components each have only a single vertex of degree greater than 1: see Figure 3.

Note that the sizes of clique edge covers and star forest decompositions are saturated below by the intersection number and star arboricity, respectively.

Theorem 4 Given a coherence graph $G_\sigma = (V, E, \sigma)$, Algorithm 1 produces $V' \models G_\sigma$.

Proof It suffices to show that $\varepsilon(v', w') = \sigma_0(\iota(v'), \iota(w'))$ via a case analysis.

First, suppose that $\sigma_0(\iota(v'), \iota(w')) = 1$: here, we need to show that v' and w' are consistent. The respective formulas $\phi(\iota(v'))$ and $\phi(\iota(w'))$ only share common variables in clauses of the form $(q_j \Rightarrow p(v'))$ and $(q_j \Rightarrow p(w'))$. These formulas and their natural language expressions are both consistent unless $p(v') = \neg p(w')$, which can only occur if $\sigma_0(\iota(v'), \iota(w')) = -1$, a contradiction.

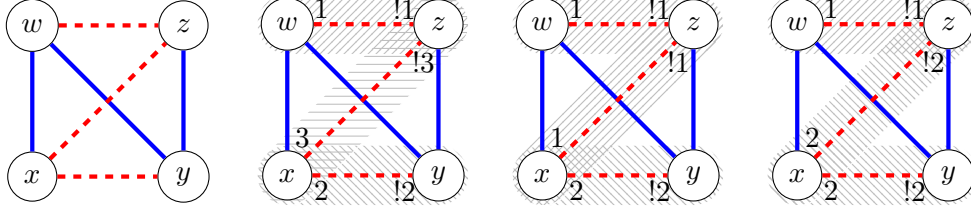


Figure 3: Left: a clique in a larger notional coherence graph. Center left: the degenerate star forest decomposition of negative edges yields the greatest number of corresponding properties. The notations n and $!n$ respectively indicate inconsistent propositional clauses of the form $(q \Rightarrow p_n)$ and $(q \Rightarrow \neg p_n)$. For example, if $\Rightarrow p_1$, $\Rightarrow p_2$, and $\Rightarrow p_3$ respectively correspond to “is hot,” “is bright,” and “is loud,” then a natural language expression of modeling propositions is $\{w' : (q \text{ is hot}), x' : (q \text{ is bright AND loud}), y' : (q \text{ is dark}), z' : (q \text{ is cold AND quiet})\}$. Right panels: the two star forest decompositions of minimal size yield the minimal number of corresponding properties. The panel on the right corresponds to $\{w' : (q \text{ is hot}), x' : (q \text{ is bright}), y' : (q \text{ is dark}), z' : (q \text{ is cold AND dark})\}$.

Next, suppose that $\sigma_0(\iota(v'), \iota(w')) = 0$: here, we need to show that v' and w' are independent. Now $\iota(v')$ and $\iota(w')$ are not in a common clique, so the respective formulas $\phi(\iota(v'))$ and $\phi(\iota(w'))$ do not share any common variables. The required result follows.

Finally, suppose that $\sigma_0(\iota(v'), \iota(w')) = -1$: here, we need to show that v' and w' are inconsistent. Now the formulas $\phi(\iota(v'))$ and $\phi(\iota(w'))$ respectively contain clauses of the form $(q_j \Rightarrow p_k)$ and $(q_j \Rightarrow \neg p_k)$ for some clique C_j and star forest F_k in the graph induced by E_j^- . Thus both the formulas and their natural language expressions are inconsistent. ■

Note that Algorithm 1 does not require a specific construction for clique edge covers or for star forest decompositions. Different constructions affect the numbers of variables and properties: see §D for different clique edge cover approaches. While the approach of Conte et al. (2020) gives practical linear-time performance for clique edge covers on graphs of thousands to millions of vertices, we deal with smaller graphs and we can therefore employ more pedestrian techniques:

- **degenerate**: take the degenerate clique edge cover formed by individual edges;
- **percolation**: find all maximal cliques, then use a constraint solver to optimize a clique edge cover (see <https://stackoverflow.com/a/49145938>);
- **partition**: initialize $G' = G$, then greedily partition $E(G')$ by iteratively removing edges from the largest clique, as discussed in but avoided by Conte et al. (2020).

Note that the first and last of these techniques actually yield a clique edge partition.

Meanwhile, practical algorithms are in shorter supply for star forest decompositions. Finding small decompositions is NP-complete (Hakimi et al., 1996). An integer linear program for star decompositions (that must be aggregated into star forest decompositions) is described in (Hajebi and Javadi, 2024), while (Cicalese and Laber, 2021) gives a linear time (1/2)-approximation algorithm for the largest minimum star size. Meanwhile, given an arboricity-realizing algorithm such as

Algorithm 1 MODELCOHERENCEGRAPH(G_σ)

Require: Coherence graph G_σ

```

1: Produce a clique edge cover  $C = \{C_1, \dots, C_m\}$  of  $G_\sigma$ 
2: for  $v \in V = V(G_\sigma)$  do
3:    $\phi(v) \leftarrow \emptyset$  // initialize with empty propositional formula
4: for  $C_j \in C$  do
5:    $E_j^- \leftarrow \{(v, w) \in E(C_j) : \sigma(v, w) = -1\}$ 
6:   Produce a star forest decomposition  $F = \{F_1, \dots, F_n\}$  of the graph induced by  $E_j^-$ 
7:   for  $F_k \in F$  do
8:     for each star  $S$  in  $F_k$  do
9:        $r \leftarrow$  root of  $S$ 
10:       $\phi(r) \leftarrow \phi(r) \wedge (q_j \Rightarrow p_k)$  // "...AND  $q_j$  has property  $p_k$ "
11:      for each leaf vertex  $\ell \in S$  do
12:         $\phi(\ell) \leftarrow \phi(\ell) \wedge (q_j \Rightarrow \neg p_k)$  // "...AND  $q_j$  has property NOT( $p_k$ )"
13: for  $v \in V$  do
14:   if  $\phi(v) = \emptyset$  then
15:      $\phi(v) \leftarrow (q_v^* \Rightarrow p_v^*)$  // to avoid triviality;  $q_v^*$  only appears in  $\phi(v)$ 
16:      $v' \leftarrow$  natural language expression of  $\phi(v)$  // see comments above
17:      $\iota(v') \leftarrow v$ 
Ensure:  $\{\iota^{-1}(v) : v \in V\} = V' \models G_\sigma$ 

```

(Gabow and Westermann, 1988), we get a (1/2)-approximate star arboricity-realizing algorithm by the observation of (Alon et al., 1992) that any tree can be covered by two star forests. The following techniques can be applied, though here we only use the second:

- take the degenerate star forest decomposition formed by individual edges;
- use the (1/2)-approximate algorithm for the largest minimum star size;
- repeatedly generate uniformly random edge partitions (Stam, 1983) and test that they contain no triangles or simple paths of (edge) length 3 (Aider et al., 2019): this is a viable brute force strategy for connected components on up to about 10 vertices since the corresponding number of partitions—i.e., the Bell number B_{10} —is 115975.

2.2. Benchmarking coherence

Because computing coherence amounts to solving MAX-CUT (or MAX-SAT more generally as in §A.2), benchmarking CDI is mainly a question of fidelity of coherence graph reconstruction. Runtime and approximation performance of combinatorial optimization algorithms in §A may become important, but at scales considered here, exact solutions are always computationally feasible.³

3. Inferring a coherence graph from a set of propositions is similar to classical natural language inference or textual entailment (Korman et al., 2018), which involves evaluating the logical relationship between two sentences (see §E). However, explanatory coherence describes more general properties of individual propositions and sets of propositions in the context of theory formation. Further, coherence encompasses a range of relations that include deductive entailment but also explanatory, analogical, perceptual, conceptual, and deliberative relations (Thagard, 2002).

The propositions we generate for our benchmarking process use a grammar that can represent multiple types of relations, as well as uncertainty about a given assignment (see §3.1). We note that the specific syntax used to represent propositions in the benchmark dataset is a matter of convenience, and users of the coherence benchmarking process can represent synthetic propositions using any syntax that is suitable for their application.

We use a “micro” F_1 score to evaluate fidelity of coherence graph reconstruction for each attempt. This accounts for class imbalance among the values in $\{-1, 0, 1\}$ for each entry in each synthetic adjacency matrix included in our evaluation task (Opitz, 2024).⁴

3. Experimental setup

We include proprietary and open-source models intentionally designed for reasoning in our evaluation. We refer to `o1-mini` (Jaech et al., 2024), `QwQ-32B` (Qwen, 2024), and `Sky-T1-32B` (NovaSky, 2025) as large reasoning models (LRMs), following the phrasing of Valmeekam et al. (2024) to describe models designed to generate long chains of thought at inference time. These models have high latency and inference costs (Abdin et al., 2024). We consider `phi-4` (Abdin et al., 2024) a small language model (SLM). We refer to the other models in our evaluation by the more generic term LLM: `gemini-2.0-flash-exp` (DeepMind, 2024), `claude-3.5-sonnet` (Anthropic, 2024), `gpt-4o` (Hurst et al., 2024), `Llama-3.3-70B` (Meta, 2024), and `gemini-1.5-pro` (Pichai and Hassabis, 2024). For all models, we performed post-processing on outputs to extract structured data for evaluation.

3.1. Adding uncertainty to propositions

To evaluate model judgments of consistency under uncertainty, we borrow from Ragin (2006). We introduce uncertainty to p or $\neg p$ by sampling from triangular fuzzy membership functions defined over the unit interval, with 1 and 0 respectively corresponding to p and $\neg p$. After adding uncertainty, a given p -assignment is syntactically represented as something like $0.619 * p$, while a given $\neg p$ assignment is syntactically represented as something like $0.346 * p$. That is, we indicate uncertainty as in the right panels of Figures 4 and 5, with results in Table 1: meanwhile, the prompt in §G echoes this construction. With $p \leftarrow \alpha * p$ and $\neg p \leftarrow \alpha_{\neg} * p$ we delineate three uncertainty regimes. The `low` regime has $\alpha \in [0.75, 1]$ and $\alpha_{\neg} \in [0, 0.25]$; the `medium` regime has $\alpha \in [0.625, 0.75]$ and $\alpha_{\neg} \in [0.25, 0.375]$, and the `high` regime has $\alpha \in [0.5, 0.625]$ and $\alpha_{\neg} \in [0.375, 0.5]$.

Encoding numerical uncertainty in natural language in a way that ensures accurate interpretation is complicated by individual differences in interpretation related to terms such as “approximately,” “certainly,” “about,” “exactly,” etc. (Krisper et al., 2019; Ferson et al., 2015). This presents a challenge for, e.g., communicating risks related to climate change, risks of developing complications from medical treatment, or the likelihood of a given geopolitical event in the future (DNI, 2015). The fuzzy set method above encodes diverse qualitative statements with a consistent formalism, and is directly relevant for use with words of estimative probability (DNI, 2015; Kachynskiy, 2019).

4. Another approach to gauging performance is to use a distance measure, as in §H. The reconstruction of a coherence graph G_{σ} is automatically of the form $G'_{\sigma'}$, where $V(G_{\sigma}) = V(G'_{\sigma'})$. Therefore, it is easy and appropriate to use the metric $d(G_{\sigma}, G'_{\sigma'}) := \|A(G_{\sigma}) - A(G'_{\sigma'})\|_1$, where adjacency matrices are indicated, and we permit $A(\cdot) \in [-1, 1]$ here for the sake of generality. This coincides with a graph edit distance in which edge insertion and deletion costs are the absolute value of the edge weight, and in which edge substitution costs are the absolute value of the difference of edge weights. Normalizing this by $|V| \cdot (|V| - 1)/2$ gives a size-independent gauge of performance.

3.2. Benchmark generation

To instantiate our benchmark, we sample coherence graphs from an Erdős-Rényi (ER) distribution. We ensure that each sample graph is fully connected by joining sampled graphs to a minimum spanning tree generated for a complete graph of equivalent size with random edge weights.

We generate 76 graphs with $|V| \in \{5, \dots, 23\}$ and tune the ER sampling parameters to target two regimes of edge density $:= |E|/\binom{|V|}{2}$: sparse has a median edge density of 0.202 and dense has a median edge density of 0.734.

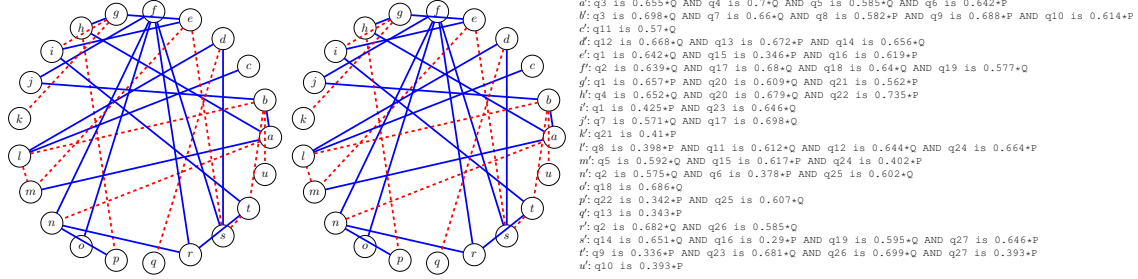


Figure 4: Left: a coherence graph from our benchmark with edge density target 0.15 (“sparse”). Center: `o1-mini` achieved perfect reconstruction on this example under high uncertainty. Right: the modeling propositions incorporated high uncertainty.

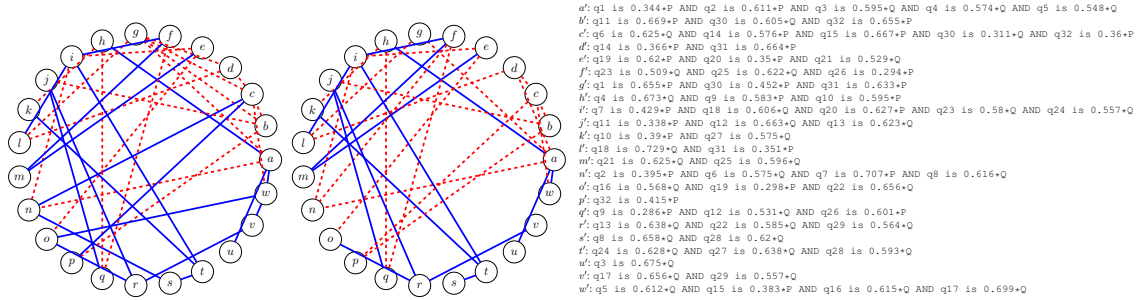


Figure 5: Left: another coherence graph from our benchmark with edge density target 0.15 (“sparse”). Center: `o1-mini` achieved good but imperfect ($F_1 = 0.96$: see vertices $c, d, g, n,$ and o) reconstruction on this example under high uncertainty. Right: the modeling propositions incorporated high uncertainty.

This yields proposition sets involving a range of variable and property counts as enumerated in §F. For each problem, we generate four additional sets of propositions. Three of these correspond to the noise regimes described above. We also generate a set of propositions where we add no noise (i.e., $p \leftarrow 1 * p$ and $\neg p \leftarrow 0 * P$) in order to control for the presence of distractors in the evaluation.

Figure 4 shows an example problem from the benchmark including a synthetic coherence graph with 21 nodes, propositions synthesized for the graph, and `o1-mini`’s perfect reconstruction of the input graph. Figure 5 is similar, but the reconstruction is imperfect.

3.3. Prompts

We use a common prompt structure shown in §G that a) establishes the consistency reasoning task, b) describes the variables and properties relevant for evaluating a set of propositions, c) establishes fuzzy membership thresholds for properties and d) embeds propositions for a given problem.

4. Results

4.1. LLMs successfully infer synthetic coherence graphs from a single prompt

Model performance varies considerably, with `o1-mini`, `claude-3.5-sonnet` and `QwQ-32B` outperforming the other models for both sparse and dense problems: see Figure 6.

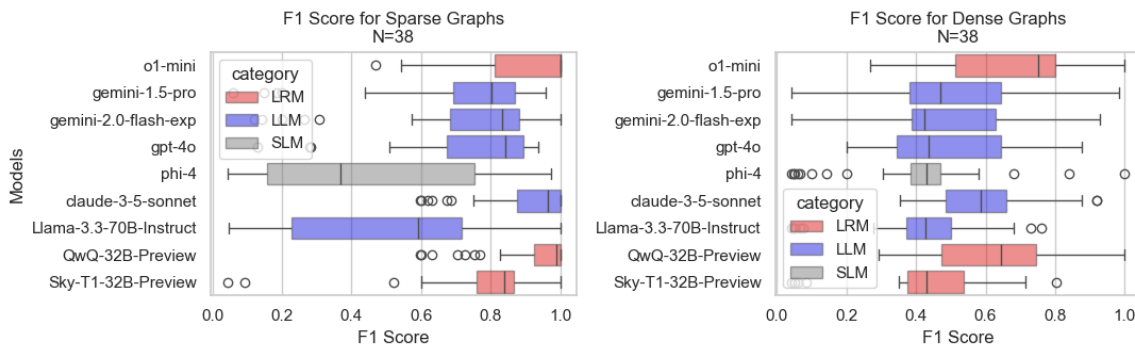


Figure 6: `o1-mini`, `claude-3.5-sonnet`, and `QwQ-32B` have high micro F_1 scores.

4.2. LLMs successfully infer synthetic coherence graphs under uncertainty

Table 1 shows that introducing uncertainty does not degrade graph reconstruction fidelity.

In Figure 7, we show how recursively passing an inferred uncertain coherence graph to `o1-mini` and prompting it to assign weights reflective of the level of uncertainty in property assignments can yield a weighted coherence graph with appropriate edge weights (less certain assignments yield smaller magnitude weights; more certain assignments yield larger magnitude weights).

4.3. Minor post-processing is sometimes necessary to handle obvious reconstruction errors

We noted four general types of reconstruction errors. First, some reconstructed graphs do not include a given proposition seen in the prompt. We observed this sporadically in all models. Second, we noticed some instances with Gemini models where the reconstructed graph contains nodes named, for instance, "Proposition(a)" instead of a or "(a)" instead of a. We noticed instances where `QwQ` incorrectly capitalized proposition names, for instance, substituting "A" for "a". We correct these first three error types in post-processing before evaluation.

Finally, we observed that some models hallucinate extra propositions in the reconstructed graph. Out of 608 inference attempts, `gemin-2.0-flash-exp` hallucinates on 10 inference attempts, `gpt-4o` on 5, `gemin-1.5-pro` on 4, and `Sky-T1-32B` on 1. We do not correct this type of error with post-processing; we instead eliminate these inference attempts from evaluation for these models since these hallucinations can be easily detected at runtime.

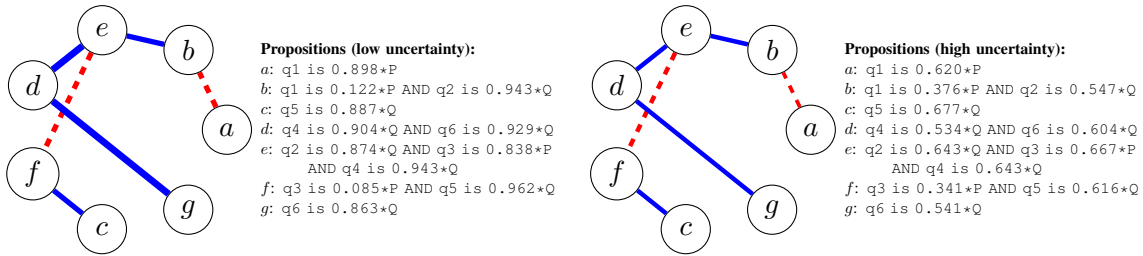


Figure 7: o1-mini-inferred weights have larger magnitude (indicated by edge thickness) when uncertainty is lower (as in the left panel). Both left and right panels reflect perfect reconstructions of the underlying graph.

model	sparsity	base case	zero unc.	low unc.	med unc.	high unc.
o1-mini	sparse	0.90 ± 0.17	0.89 ± 0.16	0.89 ± 0.15	0.89 ± 0.15	0.90 ± 0.16
	dense	0.69 ± 0.18	0.65 ± 0.19	0.63 ± 0.17	0.67 ± 0.18	0.68 ± 0.18
Gemini 1.5	sparse	0.73 ± 0.22	0.74 ± 0.24	0.78 ± 0.18	0.82 ± 0.15	0.82 ± 0.15
	dense	0.49 ± 0.19	0.48 ± 0.19	0.46 ± 0.19	0.52 ± 0.18	0.52 ± 0.16
Gemini 2.0	sparse	0.73 ± 0.24	0.68 ± 0.25	0.71 ± 0.25	0.73 ± 0.23	0.71 ± 0.27
	dense	0.49 ± 0.19	0.43 ± 0.16	0.44 ± 0.18	0.48 ± 0.17	0.49 ± 0.15
GPT-4o	sparse	0.76 ± 0.20	0.77 ± 0.18	0.77 ± 0.22	0.76 ± 0.19	0.76 ± 0.18
	dense	0.50 ± 0.19	0.47 ± 0.18	0.44 ± 0.19	0.50 ± 0.22	0.48 ± 0.19
Phi-4	sparse	0.46 ± 0.32	0.38 ± 0.33	0.36 ± 0.30	0.35 ± 0.31	0.36 ± 0.28
	dense	0.40 ± 0.21	0.40 ± 0.20	0.38 ± 0.20	0.42 ± 0.21	0.43 ± 0.20
Claude 3.5	sparse	0.90 ± 0.14	0.90 ± 0.14	0.89 ± 0.15	0.90 ± 0.14	0.90 ± 0.13
	dense	0.60 ± 0.14	0.59 ± 0.14	0.58 ± 0.14	0.60 ± 0.15	0.58 ± 0.16
Llama 3.3	sparse	0.53 ± 0.28	0.51 ± 0.27	0.55 ± 0.24	0.61 ± 0.25	0.50 ± 0.28
	dense	0.41 ± 0.18	0.45 ± 0.19	0.40 ± 0.18	0.43 ± 0.17	0.40 ± 0.18
QwQ	sparse	0.92 ± 0.12	0.90 ± 0.15	0.91 ± 0.13	0.92 ± 0.13	0.92 ± 0.13
	dense	0.62 ± 0.20	0.59 ± 0.18	0.59 ± 0.21	0.61 ± 0.22	0.60 ± 0.21
Sky-T1	sparse	0.78 ± 0.20	0.67 ± 0.27	0.61 ± 0.32	0.67 ± 0.27	0.71 ± 0.26
	dense	0.43 ± 0.18	0.40 ± 0.19	0.41 ± 0.19	0.42 ± 0.20	0.41 ± 0.19

Table 1: LLMs successfully infer synthetic coherence graphs under uncertainty (unc).

5. Conclusion

CDI provides a good model for many forms of cognition, including perception and planning. Combining CDI with consistency evaluations by neural models may lead to advancements in the state of the art in these domains. Moreover, our results indicate that it is now feasible to computationally instantiate a coherence theory of truth (Young, 2024). By hard-coding conclusively established propositions, this theory can be anchored in a correspondence theory of truth (David, 2022).

Acknowledgments

Both authors thank Tejas Patel and Jim Simpson for useful exchanges, and Alexander Medeiros and Alberto Tolentino for software engineering and infrastructure support. SH also thanks George Cybenko, Neil Gerr, Ludmilla Huntsman, Rob Johnston, Michael Robinson, Benjamin Wittes, and Levent Yilmaz for useful exchanges. This research was developed with funding from the Defense Advanced Research Projects Agency (DARPA). The views, opinions and/or findings expressed are those of the author(s) and should not be interpreted as representing the official views or policies of the Department of Defense or the U.S. Government. Distribution Statement A (Approved for Public Release, Distribution Unlimited).

References

- Marah Abdin, Jyoti Aneja, Harkirat Behl, Sébastien Bubeck, Ronen Eldan, Suriya Gunasekar, Michael Harrison, Russell J Hewett, Mojan Javaheripi, Piero Kauffmann, et al. Phi-4 technical report. *arXiv preprint arXiv:2412.08905*, 2024. URL <https://arxiv.org/abs/2412.08905>.
- Méziiane Aïder, Lamia Aoudia, Mourad Baïou, A Ridha Mahjoub, and Viet Hung Nguyen. On the star forest polytope for trees and cycles. *RAIRO-Operations Research*, 53(5):1763–1773, 2019. URL <https://doi.org/10.1051/ro/2018076>.
- Jin Akiyama and Mikio Kano. Factors and factorizations of graphs—a survey. *Journal of Graph Theory*, 9(1):1–42, 1985. URL <https://doi.org/10.1002/jgt.3190090103>.
- Noga Alon, Colin McDiarmid, and Bruce Reed. Star arboricity. *Combinatorica*, 12:375–380, 1992. URL <https://doi.org/10.1007/BF01305230>.
- Anthropic. Claude 3.5 Sonnet: raising the bar for intelligence. <https://www.anthropic.com/news/claude-3-5-sonnet>, 2024. Accessed: January 2025.
- Yoshua Bengio and Nikolay Malkin. Machine learning and information theory concepts towards an AI mathematician. *Bulletin of the American Mathematical Society*, 61(3):457–469, 2024. URL <https://doi.org/10.1090/bull/1839>.
- Mark Blokpoel and Iris van Rooij. *Theoretical Modeling for Cognitive Science and Psychology*. 2024. URL <https://computationalcognitivescience.github.io/lovelace/home>.
- Tom Brown, Benjamin Mann, Nick Ryder, Melanie Subbiah, Jared D Kaplan, Prafulla Dhariwal, Arvind Neelakantan, Pranav Shyam, Girish Sastry, Amanda Askell, et al. Language models are few-shot learners. *Advances in Neural Information Processing Systems*, 33:1877–1901, 2020. URL <https://arxiv.org/abs/2005.14165>.
- Norishige Chiba and Takao Nishizeki. Arboricity and subgraph listing algorithms. *SIAM Journal on Computing*, 14(1):210–223, 1985. URL <https://doi.org/10.1137/0214017>.
- Ferdinando Cicalese and Eduardo Sany Laber. On the star decomposition of a graph: hardness results and approximation for the max–min optimization problem. *Discrete Applied Mathematics*, 289:503–515, 2021. URL <https://doi.org/10.1016/j.dam.2020.07.014>.

- Alessio Conte, Roberto Grossi, and Andrea Marino. Large-scale clique cover of real-world networks. *Information and Computation*, 270:104464, 2020. URL <https://doi.org/10.1016/j.ic.2019.104464>.
- Natalia Criado, Elizabeth Black, and Michael Luck. A coherence maximisation process for solving normative inconsistencies. *Autonomous Agents and Multi-Agent Systems*, 30:640–680, 2016. URL <https://doi.org/10.1007/s10458-015-9300-x>.
- Marian David. The correspondence theory of truth. In Edward N. Zalta, editor, *The Stanford Encyclopedia of Philosophy*. Metaphysics Research Lab, Stanford University, Summer 2022 edition, 2022. <https://plato.stanford.edu/archives/sum2022/entries/truth-correspondence/>.
- DeepMind. Gemini 2.0 Flash Experimental. <https://deepmind.google/technologies/gemini/flash/>, 2024. Accessed: January 2025.
- DNI. Intelligence community directive 203: Analytic standards. <https://irp.fas.org/dni/icd/icd-203.pdf>, January 2 2015. Director of National Intelligence.
- Paul Erdős, Adolph W Goodman, and Louis Pósa. The representation of a graph by set intersections. *Canadian Journal of Mathematics*, 18:106–112, 1966. URL <https://doi.org/10.4153/2FCJM-1966-014-3>.
- Jiazhan Feng, Ruochen Xu, Junheng Hao, Hiteshi Sharma, Yelong Shen, Dongyan Zhao, and Weizhu Chen. Language models can be deductive solvers. In *Findings of the Association for Computational Linguistics: NAACL 2024*, pages 4026–4042, 2024. URL <https://doi.org/10.18653/v1/2024.findings-naacl.254>.
- Scott Ferson, Jason O’Rawe, Andrei Antonenko, Jack Siegrist, James Mickley, Christian C Luhmann, Kari Sentz, and Adam M Finkel. Natural language of uncertainty: numeric hedge words. *International Journal of Approximate Reasoning*, 57:19–39, 2015. URL <https://doi.org/10.1016/j.ijar.2014.11.003>.
- William M Fogarty. Formal investigation into the circumstances surrounding the downing of Iran Air flight 655 on 3 July 1988. Technical report, US Department of Defense, 1988. URL <https://apps.dtic.mil/sti/citations/ADA203577>. See also https://en.wikisource.org/wiki/Formal_Investigation_into_the_Circumstances_Surrounding_the_Downing_of_Iran_Air_Flight_655_on_3_July_1988/Formal_Report.
- M Laura Frigotto and Alessandro Rossi. An explanatory coherence model of decision making in ill-structured problems. *Mind & Society*, 14:35–55, 2015. URL <https://doi.org/10.1007/s11299-014-0158-4>.
- Harold Gabow and Herbert Westermann. Forests, frames, and games: algorithms for matroid sums and applications. In *Proceedings of the twentieth annual ACM symposium on Theory of computing*, pages 407–421, 1988. URL <https://doi.org/10.1145/62212.62252>.
- Bernd Gärtner and Jiri Matousek. *Approximation Algorithms and Semidefinite Programming*. Springer, 2012. URL <https://doi.org/10.1007/978-3-642-22015-9>.

- Jonathan L Gross, Jay Yellen, and Mark Anderson. *Graph Theory and its Applications*. CRC, 2018. URL <https://doi.org/10.1201/9780429425134>.
- Sahab Hajebi and Ramin Javadi. Parameterized complexity of star decomposition problem. *arXiv preprint arXiv:2411.13348*, 2024. URL <https://arxiv.org/abs/2411.13348>.
- S Louis Hakimi, John Mitchem, and Edward Schmeichel. Star arboricity of graphs. *Discrete Mathematics*, 149(1-3):93–98, 1996. URL [https://doi.org/10.1016/0012-365X\(94\)00313-8](https://doi.org/10.1016/0012-365X(94)00313-8).
- Simeng Han, Hailey Schoelkopf, Yilun Zhao, Zhenting Qi, Martin Riddell, Wenfei Zhou, James Coady, David Peng, Yujie Qiao, Luke Benson, et al. FOLIO: natural language reasoning with first-order logic. *arXiv preprint arXiv:2209.00840*, 2022. URL <https://arxiv.org/abs/2209.00840>.
- Keith J Holyoak and Dan Simon. Bidirectional reasoning in decision making by constraint satisfaction. *Journal of Experimental Psychology: General*, 128(1):3, 1999. URL <https://psycnet.apa.org/doi/10.1037/0096-3445.128.1.3>.
- Steve Huntsman, August 2024. URL <https://github.com/SteveHuntsman/LegalCoherence/tree/main/Vincennes>. Accessed: February 2025.
- Steve Huntsman, Michael Robinson, and Ludmilla Huntsman. Prospects for inconsistency detection using large language models and sheaves. *arXiv preprint arXiv:2401.16713*, 2024. URL <https://arxiv.org/abs/2401.16713>.
- Aaron Hurst, Adam Lerer, Adam P Goucher, Adam Perelman, Aditya Ramesh, Aidan Clark, AJ Ostrow, Akila Welihinda, Alan Hayes, Alec Radford, et al. GPT-4o system card. *arXiv preprint arXiv:2410.21276*, 2024. URL <https://arxiv.org/abs/2410.21276>.
- Aaron Jaech, Adam Kalai, Adam Lerer, Adam Richardson, Ahmed El-Kishky, Aiden Low, Alec Helyar, Aleksander Madry, Alex Beutel, Alex Carney, et al. OpenAI o1 system card. *arXiv preprint arXiv:2412.16720*, 2024. URL <https://arxiv.org/abs/2412.16720>.
- Stephen P Jordan, Noah Shutty, Mary Wootters, Adam Zalcman, Alexander Schmidhuber, Robbie King, Sergei V Isakov, and Ryan Babbush. Optimization by decoded quantum interferometry. *arXiv preprint arXiv:2408.08292*, 2024. URL <https://arxiv.org/abs/2408.08292>.
- Sindhu Joseph and Henry Prakken. Coherence-driven argumentation to norm consensus. In *Proceedings of the 12th International Conference on Artificial Intelligence and Law*, pages 58–67, 2009. URL <https://doi.org/10.1145/1568234.1568242>.
- Anatoly Kachynskiy. National security assessment method based on fuzzy sets theory. *Theoretical and Applied Cybersecurity*, 1(1), 2019. URL <https://doi.org/10.20535/tacs.2664-29132019.1.169084>.
- Daniel Kahneman. *Thinking, Fast and Slow*. Farrar, Straus and Giroux, 2011.
- Vedant Khandelwal, Vishal Pallagani, Biplav Srivastava, and Francesca Rossi. A neurosymbolic fast and slow architecture for graph coloring. *arXiv preprint arXiv:2412.01752*, 2024. URL <https://arxiv.org/abs/2412.01752>.

- Subhash Khot, Guy Kindler, Elchanan Mossel, and Ryan ODonnell. Optimal inapproximability results for MAX-CUT and other 2-variable CSPs? *SIAM Journal on Computing*, 37(1):319–357, 2007. URL <https://doi.org/10.1137/S0097539705447372>.
- Daniel Z Korman, Eric Mack, Jacob Jett, and Allen H Renear. Defining textual entailment. *Journal of the Association for Information Science and Technology*, 69(6):763–772, 2018. URL <https://doi.org/10.1002/asi.24007>.
- Jomon Kottarathil, Sudev Naduvath, and Joseph Varghese Kureethara. *Graph Theory and Decomposition*. CRC, 2024. URL <https://doi.org/10.1201/9781003391678>.
- Michael Krisper, Jürgen Dobaj, and Georg Macher. Patterns for communicating numerical uncertainty. In *Proceedings of the 24th European Conference on Pattern Languages of Programs*, pages 1–15, 2019. URL <https://doi.org/10.1145/3361149.3361160>.
- Bimal Kumar and Dmitri Roussinov. NLP-based regulatory compliance—using GPT 4.0 to decode regulatory documents. *arXiv preprint arXiv:2412.20602*, 2024. URL <https://arxiv.org/abs/2412.20602>.
- Arthur Lee and Bruce Xu. Classifying approximation algorithms: understanding the APX complexity class. *arXiv preprint arXiv:2111.01551*, 2021. URL <https://arxiv.org/abs/2111.01551>.
- Doug Lenat and Gary Marcus. Getting from generative AI to trustworthy AI: What LLMs might learn from Cyc. *arXiv preprint arXiv:2308.04445*, 2023. URL <https://arxiv.org/abs/2308.04445>.
- Chu Min Li, Felip Manyà, Joan Ramon Soler, and Amanda Vidal. Clausal forms in MaxSAT and MinSAT. *International Journal of Computational Intelligence Systems*, 15(1):97, 2022. URL <https://doi.org/10.1007/s44196-022-00143-z>.
- Jiacheng Liu, Sewon Min, Luke Zettlemoyer, Yejin Choi, and Hannaneh Hajishirzi. Infinigram: scaling unbounded n -gram language models to a trillion tokens. *arXiv preprint arXiv:2401.17377*, 2024. URL <https://arxiv.org/abs/2401.17377>.
- Maximilian Maier, Noah van Dongen, and Denny Borsboom. Comparing theories with the Ising model of explanatory coherence. *Psychological Methods*, 2023. URL <https://doi.org/10.1037/met0000543>.
- Giuseppe Marra, Sebastijan Dumančić, Robin Manhaeve, and Luc De Raedt. From statistical relational to neurosymbolic artificial intelligence: a survey. *Artificial Intelligence*, page 104062, 2024. URL <https://doi.org/10.1016/j.artint.2023.104062>.
- William Merrill and Ashish Sabharwal. The expressive power of transformers with chain of thought. In *The Twelfth International Conference on Learning Representations*, 2024. URL <https://arxiv.org/abs/2310.07923>.
- Meta. The Meta Llama 3.3 multilingual large language model (LLM). https://github.com/meta-llama/llama-models/blob/main/models/llama3_3/MODEL_CARD.md, 2024. Accessed: January 2025.

- Marc Mezard and Andrea Montanari. *Information, Physics, and Computation*. Oxford, 2009. URL <https://doi.org/10.1093/acprof:oso/9780198570837.001.0001>.
- Cristopher Moore and Stephan Mertens. *The Nature of Computation*. Oxford, 2011. URL <https://doi.org/10.1093/acprof:oso/9780199233212.001.0001>.
- Neel Nanda, Lawrence Chan, Tom Lieberum, Jess Smith, and Jacob Steinhardt. Progress measures for grokking via mechanistic interpretability. In *The Eleventh International Conference on Learning Representations*, 2023. URL <https://openreview.net/forum?id=9XFSbDPmdW>.
- Balas Kausik Natarajan. Sparse approximate solutions to linear systems. *SIAM Journal on Computing*, 24(2):227–234, 1995. URL <https://doi.org/10.1137/S0097539792240406>.
- NovaSky. Sky-T1: fully open-source reasoning model with o1-preview performance in \$450 budget, 2025. URL <https://novasky-ai.github.io/posts/sky-t1>. Accessed: January 2025.
- Franz Nowak, Anej Svete, Alexandra Butoi, and Ryan Cotterell. On the representational capacity of neural language models with chain-of-thought reasoning. *arXiv preprint arXiv:2406.14197*, 2024. URL <https://arxiv.org/abs/2406.14197>.
- Theo Olausson, Alex Gu, Ben Lipkin, Cedegao Zhang, Armando Solar-Lezama, Joshua Tenenbaum, and Roger Levy. LINC: a neurosymbolic approach for logical reasoning by combining language models with first-order logic provers. In *Proceedings of the 2023 Conference on Empirical Methods in Natural Language Processing*, pages 5153–5176, 2023. URL <https://doi.org/10.18653/v1/2023.emnlp-main.313>.
- Juri Opitz. A closer look at classification evaluation metrics and a critical reflection of common evaluation practice. *Transactions of the Association for Computational Linguistics*, 12:820–836, 2024. URL https://doi.org/10.1162/tacl_a_00675.
- Liangming Pan, Alon Albalak, Xinyi Wang, and William Wang. Logic-LM: empowering large language models with symbolic solvers for faithful logical reasoning. In *Findings of the Association for Computational Linguistics: EMNLP 2023*, pages 3806–3824, 2023. URL <https://doi.org/10.18653/v1/2023.findings-emnlp.248>.
- Binghui Peng, Srini Narayanan, and Christos Papadimitriou. On limitations of the transformer architecture. In *Conference on Language Models*, 2024. URL <https://arxiv.org/abs/2402.08164>.
- Jorge Pérez, Pablo Barceló, and Javier Marinkovic. Attention is Turing-complete. *Journal of Machine Learning Research*, 22(75):1–35, 2021. URL <https://www.jmlr.org/papers/v22/20-302.html>.
- Sundar Pichai and Demis Hassabis. Our next-generation model: Gemini 1.5, February 2024. URL <https://blog.google/technology/ai/google-gemini-next-generation-model-february-2024/>. Accessed: January 2025.

- Qwen. QwQ: reflect deeply on the boundaries of the unknown, November 2024. URL <https://qwenlm.github.io/blog/qwq-32b-preview/>. Accessed: February 2025.
- Charles C Ragin. Set relations in social research: evaluating their consistency and coverage. *Political Analysis*, 14(3):291–310, 2006. URL <https://doi.org/10.1093/pan/mpj019>.
- Nived Rajaraman, Marco Bondaschi, Ashok Vardhan Makkuva, Kannan Ramchandran, and Michael Gastpar. Transformers on Markov data: constant depth suffices. In *The Thirty-eighth Annual Conference on Neural Information Processing Systems*, 2024. URL <https://arxiv.org/abs/2407.17686>.
- Nils Reimers and Iryna Gurevych. Sentence-BERT: sentence embeddings using Siamese BERT-networks, 2019. URL <https://arxiv.org/abs/1908.10084>.
- Daniel Rosiak. *Sheaf Theory Through Examples*. MIT, 2022. URL <https://doi.org/10.7551/mitpress/12581.001.0001>.
- Amitabha Roy. Fault tolerant Boolean satisfiability. *Journal of Artificial Intelligence Research*, 25: 503–527, 2006. URL <https://doi.org/10.1613/jair.1914>.
- Abulhair Saparov and He He. Language models are greedy reasoners: a systematic formal analysis of chain-of-thought. In *The Eleventh International Conference on Learning Representations*, 2023. URL <https://arxiv.org/abs/2210.01240>.
- Md Kamruzzaman Sarker, Lu Zhou, Aaron Eberhart, and Pascal Hitzler. Neuro-symbolic artificial intelligence: current trends. *AI Communications*, 34(3):197–209, 2022. URL <https://doi.org/10.3233/AIC-210084>.
- Lesia Semenova, Cynthia Rudin, and Ronald Parr. On the existence of simpler machine learning models. In *Proceedings of the 2022 ACM Conference on Fairness, Accountability, and Transparency*, pages 1827–1858, 2022. URL <https://doi.org/10.1145/3531146.3533232>.
- Damien Sileo. tasksource: A large collection of NLP tasks with a structured dataset preprocessing framework. In *Proceedings of the 2024 Joint International Conference on Computational Linguistics, Language Resources and Evaluation (LREC-COLING 2024)*, pages 15655–15684, Torino, Italia, May 2024. ELRA and ICCL. URL <https://aclanthology.org/2024.lrec-main.1361>.
- Dan Simon. A third view of the black box: cognitive coherence in legal decision making. *University of Chicago Law Review*, 71(2):511, 2004. URL <https://chicagounbound.uchicago.edu/uclrev/vol71/iss2/3/>.
- Yellamraju V Srinivas. Applications of sheaf theory in algorithm design. Technical report, Kestrel Institute, 1993. URL <https://apps.dtic.mil/sti/citations/ADA272724>.
- AJ Stam. Generation of a random partition of a finite set by an urn model. *Journal of Combinatorial Theory, Series A*, 35(2):231–240, 1983. URL [https://doi.org/10.1016/0097-3165\(83\)90009-2](https://doi.org/10.1016/0097-3165(83)90009-2).

- Paul Thagard. Adversarial problem solving: modeling an opponent using explanatory coherence. *Cognitive Science*, 16(1):123–149, 1992. URL [https://doi.org/10.1016/0364-0213\(92\)90019-Q](https://doi.org/10.1016/0364-0213(92)90019-Q).
- Paul Thagard. *Coherence in Thought and Action*. MIT, 2002. URL <https://doi.org/10.7551/mitpress/1900.001.0001>.
- Paul Thagard. Causal inference in legal decision making: explanatory coherence vs. Bayesian networks. *Applied Artificial Intelligence*, 18(3-4):231–249, 2004. URL <https://doi.org/10.1080/08839510490279861>.
- Paul Thagard and Karsten Verbeurgt. Coherence as constraint satisfaction. *Cognitive Science*, 22(1):1–24, 1998. URL [https://doi.org/10.1016/S0364-0213\(99\)80033-0](https://doi.org/10.1016/S0364-0213(99)80033-0).
- Karthik Valmeekam, Kaya Stechly, and Subbarao Kambhampati. LLMs still can’t plan; can LRM’s? A preliminary evaluation of OpenAI’s o1 on PlanBench. *arXiv preprint arXiv:2409.13373*, 2024. URL <https://arxiv.org/abs/2409.13373>.
- Ashish Vaswani, Noam Shazeer, Niki Parmar, Jakob Uszkoreit, Llion Jones, Aidan N Gomez, Lukasz Kaiser, and Illia Polosukhin. Attention is all you need. *Advances in Neural Information Processing Systems*, 30:5998–6008, 2017. URL <https://arxiv.org/abs/1706.03762>.
- Vijay V Vazirani. *Approximation Algorithms*. Springer, 2001. URL <https://doi.org/10.1007/978-3-662-04565-7>.
- Martin J Wainwright, Elitza Maneva, and Emin Martinian. Lossy source compression using low-density generator matrix codes: analysis and algorithms. *IEEE Transactions on Information Theory*, 56(3):1351–1368, 2010. URL <https://doi.org/10.1109/TIT.2009.2039160>.
- Xi Ye, Qiaochu Chen, Isil Dillig, and Greg Durrett. SatLM: satisfiability-aided language models using declarative prompting. *Advances in Neural Information Processing Systems*, 36, 2024. URL <https://arxiv.org/abs/2305.09656>.
- Levent Yilmaz, Ana Franco-Watkins, and Timothy S Kroecker. Computational models of ethical decision-making: a coherence-driven reflective equilibrium model. *Cognitive Systems Research*, 46:61–74, 2017. URL <https://doi.org/10.1016/j.cogsys.2017.02.005>.
- James O Young. The coherence theory of truth. In Edward N. Zalta and Uri Nodelman, editors, *The Stanford Encyclopedia of Philosophy*. Metaphysics Research Lab, Stanford University, Summer 2024 edition, 2024. <https://plato.stanford.edu/archives/sum2024/entries/truth-coherence/>.
- Wanjun Zhong, Siyuan Wang, Duyu Tang, Zenan Xu, Daya Guo, Jiahai Wang, Jian Yin, Ming Zhou, and Nan Duan. AR-LSAT: investigating analytical reasoning of text. *arXiv preprint arXiv:2104.06598*, 2021. URL <https://arxiv.org/abs/2104.06598>.

Appendix A. Coherence can be computed in different ways

A.1. Classical coherence is equivalent to 2-MAX-XORSAT and to sparse approximation for 2-XORSAT

There are a number of algorithms for computing coherence classically. Besides a brute force solution to the MAX-CUT problem for a coherence graph G_σ , there are also greedy stochastic, simulated annealing, and semidefinite programming approximations (Thagard and Verbeurgt, 1998; Gärtner and Matousek, 2012). Historically, the dominant approach is a dynamical neural (“connectionist”) algorithm discussed in Thagard (2002). However, implementations are sufficiently outdated or hard to work with⁵ that an adaptation based on an Ising model has recently been developed (Maier et al., 2023).

We proceed to outline two computational perspectives on coherence that to our knowledge have not previously been considered explicitly, though the second was discussed at the level of prose in Huntsman et al. (2024). Given a coherence graph G_σ , the consistency equation $\sigma(v, w) = 1$ corresponds to an equation of the form $x_v + x_w = 0$ over the Boolean field \mathbb{F}_2 , and also to the propositional clause $v \iff w$. Meanwhile, the inconsistency equation $\sigma(v, w) = -1$ corresponds to $x_v + x_w = 1$, and also to the propositional clause $v \oplus w$, where $\oplus = \text{XOR}$. Therefore, we can repackage G_σ into the linear equation $Bx = c$, where B is the incidence matrix of G_σ , or equivalently the biadjacency matrix of the factor graph of the 2-XORSAT/2-Affine-SAT (Roy, 2006; Mezard and Montanari, 2009) formula obtained from the clauses indicated just above.

For example, the coherence graph in Figure 2 corresponds to the linear equation

$$\begin{pmatrix} 1 & 1 & 0 & 0 & 0 \\ 0 & 1 & 1 & 0 & 0 \\ 0 & 1 & 0 & 1 & 0 \\ 0 & 1 & 0 & 0 & 1 \\ 0 & 0 & 1 & 1 & 0 \\ 0 & 0 & 0 & 1 & 1 \\ 1 & 0 & 0 & 0 & 1 \end{pmatrix} \begin{pmatrix} x_a \\ x_b \\ x_c \\ x_d \\ x_e \end{pmatrix} = \begin{pmatrix} 1 \\ 0 \\ 1 \\ 0 \\ 0 \\ 1 \\ 0 \end{pmatrix}$$

and also to the propositional formula

$$(a \oplus b) \wedge (b \iff b) \wedge (b \oplus d) \wedge (b \iff e) \wedge (c \iff d) \wedge (d \oplus e) \wedge (e \iff a).$$

By using the identities $v \iff w \equiv (\neg v \vee w) \wedge (v \vee \neg w)$ and $v \oplus w \equiv (v \vee w) \wedge (\neg v \vee \neg w)$, we can transform this into a CNF-SAT formula.

Of course, in general the linear equation has no solution and the propositional formula is unsatisfiable. In the propositional context, the coherence computation corresponds to the MAX-2-XORSAT problem, which unsurprisingly reduces to MAX-CUT (Moore and Mertens, 2011). To our knowledge, the linear algebra formulation of coherence does not appear in the literature.⁶ The

5. See, e.g., <https://github.com/mars0i/popco>, https://github.com/russellcameronthomas/JavaECHO_command_line, <https://github.com/B-Sabev/ComputationalModelsOfCoherence>, <https://github.com/tjd/echo>, or <https://github.com/MaxRae/ConnectionistSudoku>. Even the two most recent of these have not been updated for six years as of this writing.

6. However, this formulation of the MAX-XORSAT problem is found in the literature on low-density generator matrix codes, where it is equivalent to performing source encoding (Wainwright et al., 2010).

goal is to find a certain approximate solution to $Bx = c$, where again B is the incidence matrix (over \mathbb{F}_2) of G_σ , x is a vector of propositional truth values, and c is a vector encoding σ . Specifically, we want to find the assignment x that satisfies the most rows of the equation: this is equivalent to satisfying the most clauses, i.e., to solving MAX-(2-XOR)SAT all over again. In the language of sparse approximation, we want to solve $\arg \min_x \|Bx - c\|_0$ over \mathbb{F}_2 , where the L^0 “norm” (i.e., the size of the support) is indicated.⁷ We can write this as a more conventional-looking optimization with objective $\sum_j (-1)^{c_j + e_j^T Bx}$ (Jordan et al., 2024). However, there is a more general formulation as an integer linear program (Vazirani, 2001) whose relaxation is of substantial practical interest, as we shall discuss in the sequel.

A.2. A general approach: weighted MAX-SAT

We sketch how to represent higher-order (in)consistency relationships such as trilemmas. A conceptually simple but computationally involved general approach is as follows:

- for each ordered pair of dependent claims, rate the consistency of the second given the first, and associate this to a weight for an implication term;
- for each ordered triple of dependent claims, rate the consistency of the second and third given the first, and separately the consistency of the third given the first and second: associate these with corresponding implication terms;
- etc., truncating this hierarchy as desired/practical.

Note that this requires a clique-finding algorithm such as that of Chiba and Nishizeki (1985), and that each unordered tuple corresponds to several ordered tuples, ensuring symmetry.

While this approach appears to adequately generalize the notion of a coherence graph into what amounts to a weighted *simplicial complex*—i.e., a weighted hypergraph containing all sub-hyperedges (Rosiak, 2022)—it is not yet suitable for practical MAX-SAT solvers of any sort. These only address weighted CNF-SAT problems, while common translations into CNF-SAT do not preserve weights correctly. Therefore, applying a MAX-SAT solver would generally require (implementing and) applying a specialized transformation of the sort detailed in Li et al. (2022), which to our knowledge has no public implementation.

Once a coherence problem is properly transformed into CNF-SAT, there is an interesting alternative to weighted MAX-SAT solvers. An efficient probabilistic algorithm for weighted MAX-SAT discussed in Vazirani (2001) provides a natural probabilistic interpretation that is certain to be useful in many if not most practical situations. For example, a proposition with acceptance probability near 0.5 may indicate a need for—and even drive the collection of—additional data for incorporation into the relevant structure.

The general approach to representing and solving “higher-order” coherence problems outlined just above was suggested by Huntsman et al. (2024), who were unaware of prior work on coherence *per se*. The underlying motivation was that a *sheaf* ought to represent consistency data. Briefly,

7. Note that i) over \mathbb{F}_2 , the L^0 and L^1 norms are the same, but this offers no advantage; and ii) the usual problem of sparse approximation is of the form $\min_y \|y\|_0$ such that $b = Ay$. Our problem is not expressible in this way and it does not appear to be treated in the literature from the perspective of sparse approximation/optimization, cf. (Natarajan, 1995).

a sheaf is comprised of data on open sets in a topological space that satisfy natural restriction—equivalently, gluing—axioms (Rosiak, 2022). The connection to sheaves is that every logical clause in a CNF-SAT formula introduces a logical constraint that must be satisfied in order for the overall formula to be satisfied. In particular, adding clauses can never enlarge the solution space (Srinivas, 1993).

It is not immediately clear how to adapt our approach for modeling coherence graphs to this more general setting. We leave this for future work.

Appendix B. A case study comparing human and LLM consistency ratings

There is additional evidence that LLMs can reliably gauge propositional (in)consistency (Huntsman et al., 2024; Kumar and Roussinov, 2024). However, we are not aware of any assessment of performance relative to humans. Here, we outline a case study performed in summer 2024 in which ChatGPT 4 demonstrated superhuman performance at gauging (in)consistency.

In Thagard (1992), a coherence graph modeled a decision facing the captain of the cruiser USS *Vincennes* on 3 July 1988: was radar track 4131 taking off from the Iranian civilian-military airfield at Bandar Abbas a civilian aircraft, or a hostile F-14 preparing to attack? The coherence graph included “positive evidence” propositions (labeled E*) copied almost verbatim from §III.C.1.b of the investigation report (Fogarty, 1988) along with a few of their negations (labeled NE*) and hypothetical propositions that the track was attacking (labeled A*) or commercial (labeled C*). As is still common today for analyses using CDI, the edge set and weights (here, simply signs) were constructed by hand.

To focus on ChatGPT 4’s performance in evaluating (in)consistency, we considered the same edge set as the manually-constructed coherence graph, i.e., we neglected any considerations of dependence.

It is important to note here that (the nontrivial connected component of) the coherence graph has $|V| = 21$ and $|E| = 36$, so its edge density is $36/210 = 0.17$. **In other words, this example is in exactly the same regime as the larger and sparser benchmark graphs discussed in the main text.**

For each edge, we asked ChatGPT 4 to rate the consistency of the corresponding pairs of propositions 10 times using a variant of the prompt in Huntsman et al. (2024) that included an extract from the executive summary of Fogarty (1988) as background information. The results are shown in Figures 8 and 9. Supporting data and scripts are in Huntsman (2024).

A bit of introspection and common sense reveals that for the largest discrepancies between the median LLM rating and the human rating, the median LLM rating is more reasonable in each event. Consider the four largest discrepancies, listed in order of their appearance in Figure 9:

A2-C2: These are obviously consistent, so ChatGPT 4’s rating is better than the rating in Thagard (1992).

- A2 is “Track 4131 was an F-14.”
- C2 is “Track 4131 was taking off.”

A3-E3: Examination of outputs shows that ChatGPT 4 considered plausible technical failures and misunderstandings. In light of this, it is fair to conclude that ChatGPT 4’s rating is better than the rating in Thagard (1992).

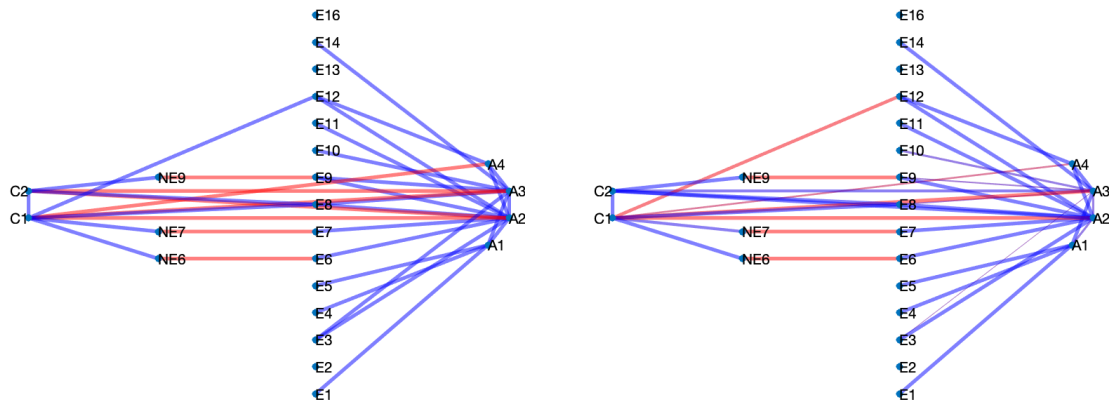


Figure 8: Left: A hand-crafted coherence graph from Thagard (1992). Blue and red respectively indicate positive and negative edge weights. Right: A coherence graph with the same edges, but with weights given by rescaled median consistency ratings from ChatGPT 4. Thickness indicates the relative magnitude of weights.

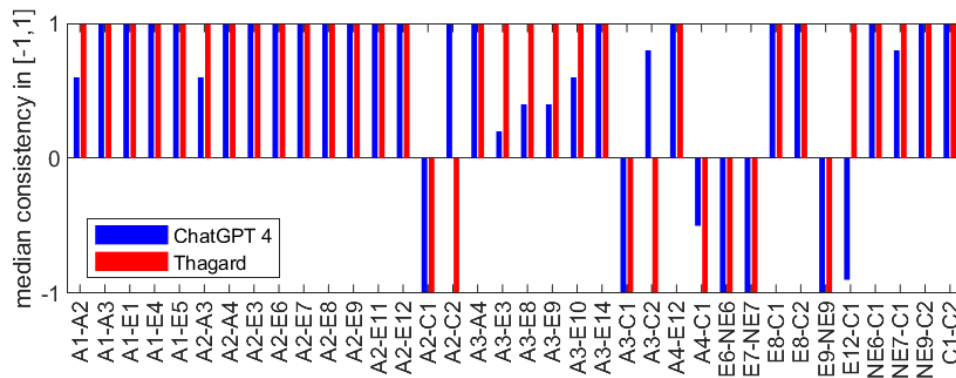


Figure 9: Rescaled median consistency ratings by ChatGPT 4 versus hand-crafted consistency ratings from Thagard (1992).

- A3 is “Track 4131 intended to attack.”
- C3 is “Track 4131 was not responding to verbal warnings over [air distress frequencies].”

A3-C2: Both A3 and C2 are listed above. These are obviously consistent, so ChatGPT 4’s rating is better than the rating in Thagard (1992).

E12-C1: Examination of outputs shows that ChatGPT 4 considered navigation and communications emissions of commercial airliners. In light of this, it is fair to conclude that ChatGPT 4’s rating is better than the rating in Thagard (1992).

- E12 is “No [electronic emissions were reported] from track 4131, however, F-14s can fly [without electronic emissions].”
- C1 is “Track 4131 was a commercial airliner.”

To summarize, ChatGPT 4 demonstrated superhuman performance at gauging the (in)consistency of propositions.

Appendix C. ANOVA for micro F_1

The two-way ANOVA for micro F_1 in Table 2 shows significant effects.

	SS	DF	F	p-value
Model	9.69	8.0	29.62	< 0.001
Sparsity	9.35	1.0	228.51	< 0.001
Model \times sparsity	1.30	8.0	3.97	< 0.001
Error	27.77	679.0	NaN	NaN

Table 2: A two-way ANOVA shows significance for model, sparsity, and their interaction.

Appendix D. Benchmark generation parameters can be altered to synthesize problem sets with desired characteristics

Figure 10 demonstrates how benchmark generation parameters lead to increasing numbers of variables in the resulting synthetic problem sets as graph sizes increase. The top row shows data for small graphs (5-11 propositions), middle row: medium graphs (13-17 propositions), bottom row: large graphs (19-23 propositions). In general, the `degenerate` edge clique processing method and the `partition` method (first and third subcolumns in each panel) lead to more variables and fewer properties than the `percolation` method (middle column of each panel).

Appendix E. Inferring logical entailment with ModernBERT fine-tuned for NLI

We performed a preliminary experiment to test whether we could directly identify either a) relevance (defined as two propositions sharing a single variable) or b) consistency directly from white box LLM embeddings or from a number of simple quantifications of inter-token attention in the

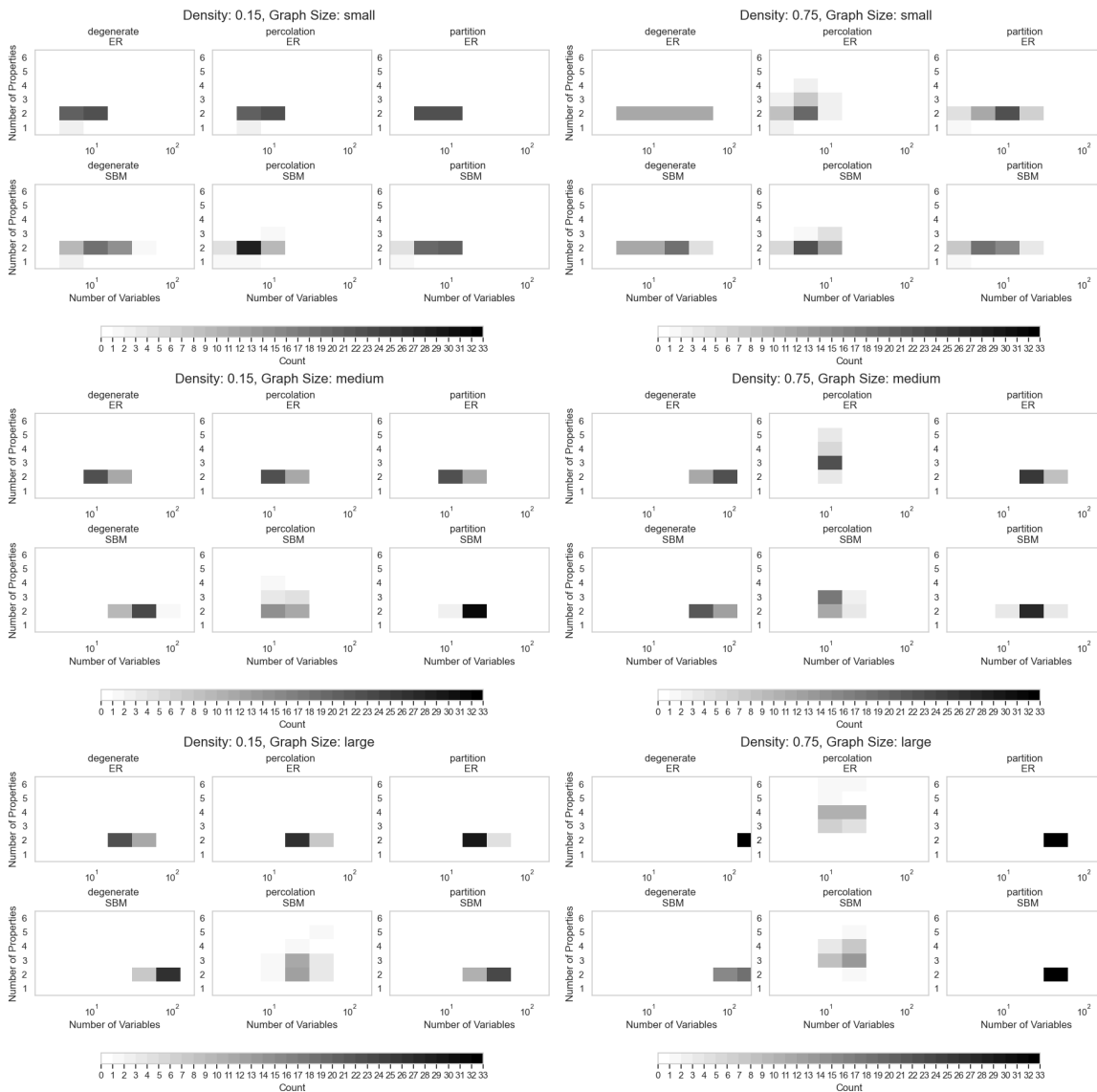


Figure 10: Figure 10 Changing benchmark generation parameters leads to increasing numbers of variables in the resulting synthetic problem sets as graph sizes increase. Top row: small graphs (5-11 propositions). Middle row: medium graphs (13-17 propositions). Bottom row: large graphs (19-23 props). In general, the degenerate edge clique processing method and the partition method (first and third subcolumns in each panel) lead to more variables and fewer properties than the percolation method (middle column of each panel).

models’ attention mechanisms. While these experiments showed a consistently high error rate (suggesting the need for a more sophisticated mechanistic interpretability study along the lines described by Nanda et al. 2023) we report the best results, which came from using a small BERT model (ModernBERT fine-tuned to infer entailment relations between propositions (Sileo, 2024; Reimers and Gurevych, 2019).

Using propositions in the simplified natural language grammar of our benchmark shows accurate entailment inferences along the diagonal (left figure), but multiple errors in off-diagonal relations (e.g., inferring a contradiction in (2,4) between “ q_2 is !P” and “ q_4 is !P”, among others). However, rewriting propositions more formally (right) shows that ModernBERT is able to perfectly infer consistency relations among these propositions.

Our tests to extract logical relations directly from attention encodings included estimating e.g., mean or median inter-token attention at the first layer, last layer, or across all layers for QwQ-32B (the most performant open source LLM for our purposes) using benchmark propositions and propositions rewritten in propositional logic. We also tested applying regression to correct positional and autoregressive attention effects. These experiments were inconclusive, suggesting that more complex statistical measures might be needed to identify reasoning mechanisms in white box models.

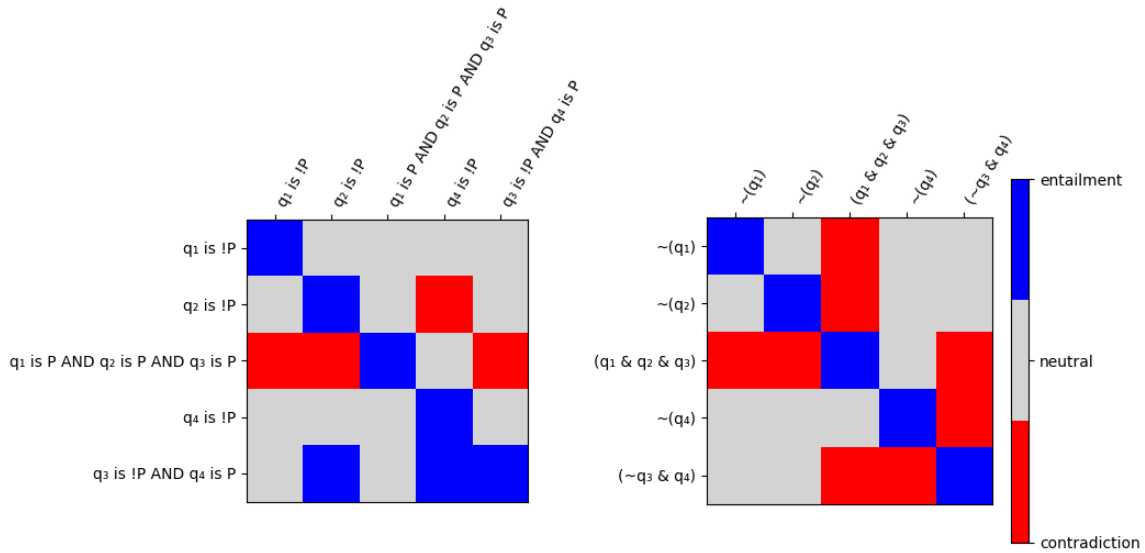


Figure 11: Pairwise natural language inference using ModernBERT for propositions of a simple one property problem shows errors on benchmark propositions (left) but perfect accuracy with propositions transformed to propositional logic (right).

Appendix F. Characteristics of synthetic coherence graphs included in our benchmark experiment

In Table 3, we show that our experiment includes coherence graphs ranging in size from 5 to 23 propositions. We note that our requirement that all synthetic coherence graphs be connected makes

harder to meet the desired sparsity (`sparse` and `dense` corresponding to target densities of 0.15 and 0.75 respectively) levels for smaller graphs (5-11 propositions).

n propositions	sparsity	n variables median	n properties median	edges median	density mean	problem count
5	<code>sparse</code>	4.0	1.5	4.0	0.400000	4
	<code>dense</code>	3.0	2.0	7.0	0.700000	4
7	<code>sparse</code>	6.0	2.0	6.0	0.285714	4
	<code>dense</code>	5.5	2.0	15.0	0.714286	4
9	<code>sparse</code>	8.0	2.0	8.0	0.222222	4
	<code>dense</code>	6.5	2.0	27.0	0.750000	4
11	<code>sparse</code>	10.0	2.0	10.0	0.181818	4
	<code>dense</code>	9.5	3.0	41.0	0.745455	4
13	<code>sparse</code>	12.0	2.0	12.0	0.153846	4
	<code>dense</code>	13.5	2.0	58.0	0.743590	4
15	<code>sparse</code>	15.0	2.0	15.0	0.142857	4
	<code>dense</code>	17.5	2.5	78.0	0.742857	4
17	<code>sparse</code>	19.0	2.0	20.0	0.147059	4
	<code>dense</code>	23.0	2.5	102.0	0.750000	4
19	<code>sparse</code>	22.0	2.0	25.0	0.146199	4
	<code>dense</code>	29.0	2.5	128.0	0.748538	4
21	<code>sparse</code>	27.0	2.0	31.0	0.147619	3
	<code>dense</code>	42.0	2.0	157.0	0.747619	3
23	<code>sparse</code>	32.0	2.0	37.0	0.146245	3
	<code>dense</code>	52.0	2.0	189.0	0.747036	3

Table 3: Our experimental benchmark includes 76 graphs (N=38 `sparse` and N=38 `dense`) ranging in size from 5 to 23 propositions.

Appendix G. Prompt template for global consistency inference under uncertainty

For the input set of propositions, identify which propositions are logically consistent (i.e., can co-exist without contradiction). Construct a networkx graph where inconsistent edges are weight 1 and consistent edges are weight 0. If two vertices do not involve the same variables, do not create an edge between them.

Return solely the edge list with proposition names for vertices. i.e., return responses in this format:

```
[('b', 'c', 0),
 ('b', 'e', 0),
 ('c', 'd', 0),
 ('c', 'e', 0)]
```

Variables:

[$'q_1'$, $'q_2'$, $'q_3'$, $'q_4'$]

A given variable can have these properties:

property P: $P \text{ XOR } !P$

property Q: $Q \text{ XOR } !Q$

property R: $R \text{ XOR } !R$

property S: $S \text{ XOR } !S$

A given property is assigned in a fuzzy manner:

property 1: $!P := < 0.5P$. $P := \geq 0.5P$

property 2: $!Q := < 0.5Q$. $Q := \geq 0.5Q$

property 3: $!R := < 0.5R$. $R := \geq 0.5R$

property 4: $!S := < 0.5S$. $S := \geq 0.5S$

Input:

[$'\text{Proposition(a): } q_1 \text{ is } !P''$,

$'\text{Proposition(b): } q_2 \text{ is } !P''$,

$'\text{Proposition(c): } q_1 \text{ is } P \text{ AND } q_2 \text{ is } P \text{ AND } q_3 \text{ is } P''$,

$'\text{Proposition(d): } q_4 \text{ is } !P''$,

$'\text{Proposition(e): } q_3 \text{ is } !P \text{ AND } q_4 \text{ is } P''$]

Appendix H. Fidelity of the reconstruction of the graph measured by the L^1 norm normalized by graph size

Figure 12 shows that o1-mini, claude-3.5-sonnet and QwQ-32B-Preview out perform all other models on sparse problems if we characterize reconstruction error using the measure of adjacency matrix similarity described in §2.2.

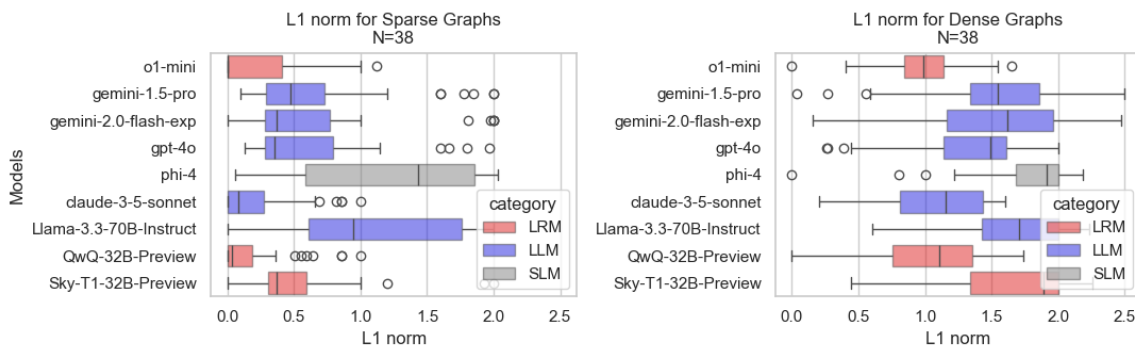


Figure 12: o1-mini, claude-3.5-sonnet, and QwQ-32B have lower (higher fidelity) L_1 scores than other models.

